



Publication Year	2019
Acceptance in OA @INAF	2020-12-03T15:26:21Z
Title	The Rocky-Like Behavior of Cometary Landslides on 67P/Churyumov-Gerasimenko
Authors	LUCCHETTI, ALICE; PENASA, LUCA; PAJOLA, MAURIZIO; MASSIRONI, MATTEO; Brunetti, Maria Teresa; et al.
DOI	10.1029/2019GL085132
Handle	http://hdl.handle.net/20.500.12386/28662
Journal	GEOPHYSICAL RESEARCH LETTERS
Number	46

Geophysical Research Letters

RESEARCH LETTER

10.1029/2019GL085132

Key Points:

- The height to runout length (H/L) of comet 67P/Churyumov-Gerasimenko landslides ranges between 0.50 and 0.97
- 67P landslides reveal a rocky-type mechanical behavior indicating that comets are made by consolidated materials
- The H/L variability is an indicator of the different volatile content located in the top few meters of the cometary crust

Supporting Information:

- Supporting Information S1

Correspondence to:

A. Lucchetti,
alice.lucchetti@inaf.it

Citation:

Lucchetti, A., Penasa, L., Pajola, M., Massironi, M., Brunetti, M. T., Cremonese, G., et al. (2019). The rocky-like behavior of cometary landslides on 67P/Churyumov-Gerasimenko. *Geophysical Research Letters*, 46, 14,336–14,346.
<https://doi.org/10.1029/2019GL085132>

Received 22 AUG 2019

Accepted 11 DEC 2019

Accepted article online 18 DEC 2019

Published online 27 DEC 2019

The Rocky-Like Behavior of Cometary Landslides on 67P/Churyumov-Gerasimenko

Alice Lucchetti¹, Luca Penasa², Maurizio Pajola¹, Matteo Massironi^{3,1,2}, Maria Teresa Brunetti⁴, Gabriele Cremonese¹, Nilda Oklay⁵, Jean-Baptiste Vincent⁵, Stefano Mottola⁵, Sonia Fornasier⁶, Holger Sierks⁷, Giampiero Naletto^{8,9,2}, Philippe L. Lamy¹⁰, Rafael Rodrigo^{11,12}, Detlef Koschny¹³, Bjorn Davidsson¹⁴, Cesare Barbieri⁸, Maria Antonietta Barucci⁶, Jean-Loup Bertaux¹⁵, Ivano Bertini⁸, Dennis Bodewits¹⁶, Pamela Cambianica², Vania Da Deppo⁹, Stefano Debei¹⁷, Mariolino De Cecco¹⁸, Jacob Deller⁷, Sabrina Ferrari², Francesca Ferri², Marco Franceschi³, Marco Fulle¹⁹, Pedro Gutiérrez²⁰, Carsten Güttler⁷, Wing-H. Ip^{21,22}, Uwe Keller^{23,5}, Luisa Lara²⁰, Monica Lazzarin⁸, Jose Lopez Moreno²⁰, Francesco Marzari⁸, and Cecilia Tubiana⁷

¹Astronomical Observatory of Padua, INAF, Padua, Italy, ²Center of Studies and Activities for Space (CISAS) “G. Colombo”, University of Padua, Padua, Italy, ³Department of Geosciences, University of Padua, Padua, Italy, ⁴Research Institute for Geo-Hydrological Protection-Italian National Research Council, Perugia, Italy, ⁵Institut für Planetenforschung, Deutsches Zentrum für Luft- und Raumfahrt (DLR), Berlin, Germany, ⁶LESIA, Observatoire de Paris, Université PSL, CNRS, Université Paris Diderot, Sorbonne Paris Cité, Sorbonne Université, Meudon, Principal Cedex, France, ⁷Max Planck Institute for Solar System Research, Göttingen, Germany, ⁸Department of Physics and Astronomy “Galileo Galilei”, University of Padua, Padua, Italy, ⁹CNR-IFN UOS Padua LUXOR, Padua, Italy, ¹⁰Laboratoire d’Astrophysique de Marseille, UMR 7326, CNRS and Aix Marseille Université, Marseille Cedex 13, France, ¹¹Centro de Astrobiología, CSIC-INTA, Madrid, Spain, ¹²International Space Science Institute, Bern, Switzerland, ¹³Science Support Office, European Space Research and Technology Centre/ESA, Noordwijk, ZH, The Netherlands, ¹⁴Jet Propulsion Laboratory, Pasadena, CA, USA, ¹⁵LATMOS, CNRS/UVSQ/IPSL, Guyancourt, France, ¹⁶Physics Department, Auburn University, Auburn, AL, USA, ¹⁷Department of Industrial Engineering, University of Padua, Padua, Italy, ¹⁸Faculty of Engineering, University of Trento, Trento, Italy, ¹⁹INAF Astronomical Observatory of Trieste, Trieste, Italy, ²⁰Instituto de Astrofísica de Andalucía (CSIC), Granada, Spain, ²¹Graduate Institute of Astronomy, National Central University, Chung-Li, Taiwan, ²²Space Science Institute, Macau University of Science and Technology, Taipa, Macau, ²³Institut für Geophysik und extraterrestrische Physik, Technische Universität Braunschweig, Braunschweig, Germany

Abstract Landslides have been identified on several solar system bodies, and different mechanisms have been proposed to explain their runout length. We analyze images from the Rosetta mission and report the global characterization of such features on comet 67P/Churyumov-Gerasimenko’s surface. By assuming the height to runout length as an approximation for the friction coefficient of landslide material, we find that on comet 67P, this ratio falls between 0.50 and 0.97. Such unexpected high values reveal a rocky-type mechanical behavior that is much more akin to Earth dry landslides than to icy satellites’ mass movements. This behavior indicates that 67P and likely comets in general are characterized by consolidated materials possibly rejecting the idea that they are fluffy aggregates. The variability of the runout length among 67P landslides can be attributed to the different volatile content located in the top few meters of the cometary crust, which can drive the mass movement.

Plain Language Summary Comet 67P Churyumov-Gerasimenko has been imaged with unprecedented spatial detail thanks to the high-resolution OSIRIS camera (Optical, Spectroscopic and Infrared Remote Imaging System) on board the Rosetta spacecraft. 67P is characterized by an extremely diverse morphology comprising different surface features such as rough consolidated terrains, smooth plains, unconsolidated mantles, pits, fractures, cliffs, cuestas, ubiquitous boulders, and layers. The peculiarity of 67P is also reflected by the widespread presence of landslides. By using high-resolution images, we analyze the shape and aspect ratio of the landslides located on comet 67P finding a mechanical behavior of the cometary material that is more akin to Earth dry landslides than to icy satellites’ mass movements. These results make 67P a very peculiar object, mainly composed by ices and refractory materials but characterized by rocky-type properties rather than icy-type characteristics. In addition, the considerable variability among the different landslides of 67P suggests that different volatile contents located in the top few meters of the cometary crust play a fundamental role on mass movement, hence being a general indicator for the subsurface cometary heterogeneities.

1. Introduction

Mass movements are almost ubiquitous in the solar system, with rockfall, avalanches, or landslides that are observed not only on Earth but also on multiple other terrestrial bodies, such as the Moon (Bart et al., 2007; Xiao et al., 2013), Mars (Lucchitta, 1987; McEwen, 1989; Quantin et al., 2004; Lucas & Mangeney, 2007; Brunetti et al., 2014; Crosta et al., 2018), Mercury (Malin & Dzurisin, 1978), Venus (Malin, 1992), the Martian moon Phobos (Shingareva & Kuzmin, 2001), Jovian moons (Schenk & Bulmer, 1998; Moore et al., 1999), Saturn moons (Singer et al., 2012), Pluto's moon Charon (Beddingfield et al., 2018), and asteroids surfaces of Vesta and Ceres (Otto et al., 2013; Schmidt et al., 2017). The characteristics of a mass transport event and, therefore, of the related accumulation material can be extremely variable. The morphology (e.g., area, volume, runout length, drop height, width, and texture) of the deposit is controlled by factors such as the initial topographic profile, the mechanism of slope failure, the mechanical properties of the collapsing material, the presence within the sliding mass of fluids and volatiles, and the specific environmental conditions (Pike, 1988; Cruden & Varnes, 1996; Hungr et al., 2014). For this reason, individual landslides might largely vary on the different bodies and on different regional sectors of the same body.

Comet 67P Churyumov-Gerasimenko (hereafter 67P) has been imaged with unprecedented spatial detail thanks to the high-resolution OSIRIS camera (Keller et al., 2007; Optical, Spectroscopic and Infrared Remote Imaging System) on board the Rosetta spacecraft. The nucleus of 67P has a bilobate shape characterized by a big and small lobe, hereafter called body and head respectively, connected by a narrow region called neck. 67P has a diameter of about 4 km (approximately 4.3 by 4.1 km at its longest and widest dimensions), a density (Preusker et al., 2017) of 537 kg m^{-3} , and a mean gravity (Sierks et al., 2015) of $2 \times 10^{-4} \text{ m s}^{-2}$. 67P is characterized by an extremely diverse morphology comprising different surface features such as rough consolidated terrains, smooth plains, unconsolidated mantles, pits, fractures, cliffs, cuestas, ubiquitous boulders, and layers (Thomas et al., 2015). The peculiarity of 67P is also reflected by the widespread presence of landslides, whose deposits are typically identified in geomorphological maps as gravitational accumulation collapses (El-Maarry et al., 2016; Giacomini et al., 2016).

This work widens the landslides data set of the solar system, and in particular on icy bodies, producing a global mapping and a detailed analysis of such surface features on a cometary nucleus. The 67P landslide analysis reveals a clear rocky-type behavior of cometary material, which is more similar to terrestrial material and totally different from what is observed on other solar system icy bodies. These results show that 67P and likely comets, in general, are characterized by consolidated material, hence rejecting the idea that they are fluffy aggregates.

2. Data Set: Identification of Landslides on Comet 67P

On 67P, multiple landslide deposits are identified in close association with cliffs. These observations suggest that cliff collapse is an important process in reshaping cometary surfaces (Britt et al., 2004; Pajola et al., 2015; Steckloff et al., 2016; Steckloff & Samarasinha, 2018). OSIRIS observations show a direct evidence of the occurrence of a cometary landslide, with the resulting production of a newly formed boulder talus located at the base of the scarp (see the Aswan case; Pajola et al., 2017). Several gravitational accumulation deposits of fragmented material have been identified on the surface of 67P associated with well-defined scarps from which the material had detached (Figure 1).

The global coverage and different viewing geometries of OSIRIS NAC (Narrow Angle Camera) and WAC (Wide Angle Camera) images allowed the identification of landslides located on different physiographic and geological regions on 67P (El-Maarry et al., 2016; Giacomini et al., 2016). The landslide database was mainly built on NAC images taken at distance of 42–80 km, corresponding to a pixel scale of 1.12–1.49 m/px that allowed us to outline the identified landslide deposits. For each landslide, multiple high-resolution (between 0.3 and 1.5 m/px) images were used to have different view of the same deposit and, hence, to confirm their identification (supporting information). We mapped 26 deposits in ESRI ArcGIS 10.3 as polygons on the surface of the comet, mainly occurring in the northern and equatorial regions of 67P (Figure 2).

We mapped well-confined deposits with a well-defined areal extent, detectable from OSIRIS images, and close to their cliff sources. We do not consider continuous nonlaterally bounded gravitational taluses at

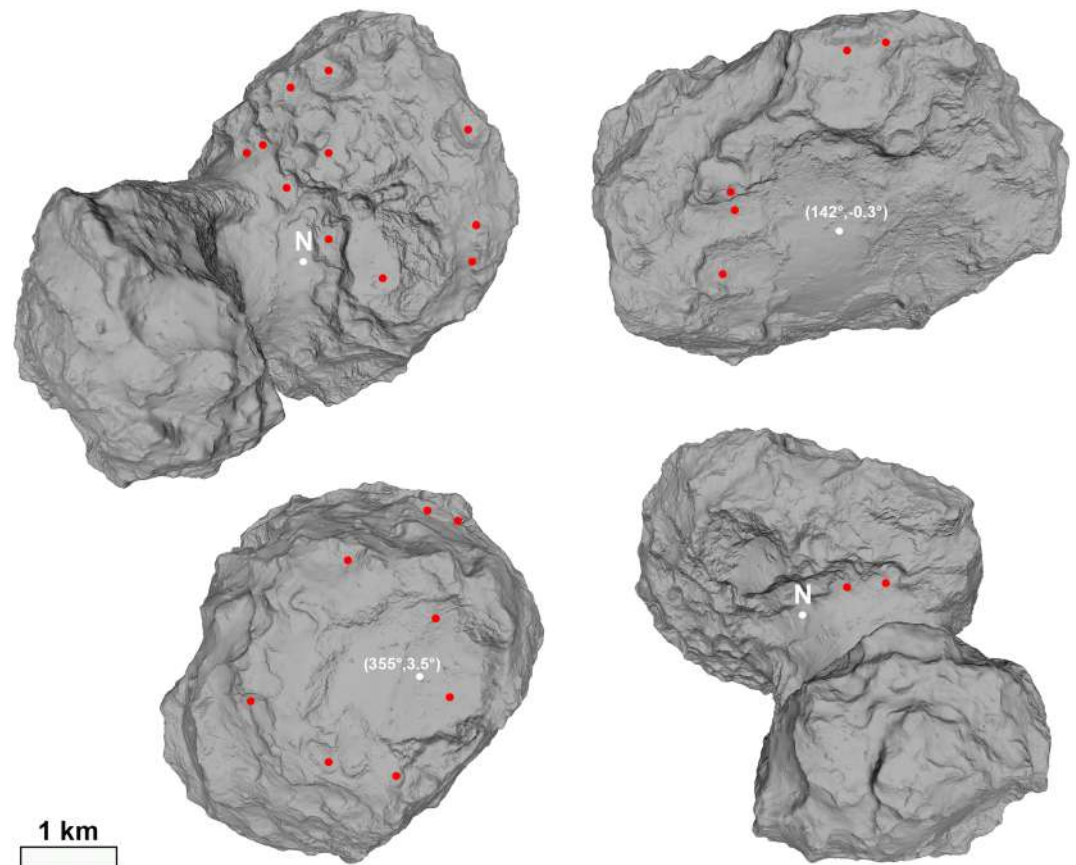


Figure 1. Global distribution of landslides on comet 67P. The 26 landslides identified on the surface of comet 67P (4 km diameter size) are mainly located on the northern hemisphere. The locations of the identified landslides are indicated with red dots, while the white dots indicate the north pole or the latitude and longitude coordinated in the Cheops reference frame (Preusker et al., 2015).

the base of the cliffs, diamictons of uncertain origin, and group of boulders at the base of the cliffs, which are not organized in well-defined accumulation deposit. For instance, for several boulders located in the southern hemisphere (Pajola et al., 2016), it was not possible to univocally associate the corresponding cliffs; hence, no landslides were identified there. This lack of landslides reflects the clear surface dichotomy characterizing the two hemispheres of 67P. Indeed, on the northern terrain large cliffs and consolidated terrains are coupled with dusty deposits and smooth terrains (Giacomini et al., 2016; Vincent et al., 2017) also due to the transport of fallback material, primarily from the southern hemisphere to the north (Lai et al., 2017), while on the southern hemisphere a much smoother topography is present and cliffs heights tend to be smaller (Vincent et al., 2017).

The morphological appearance of 67P landslides resembles rock/ice avalanches (Hungr et al., 2014), that is, a massive mass movement of bedrock broken from a destabilized slope moving in a flow-like manner (this aspect separates landslide from a pure fall), where the motion of the fragmented ice/rock is dominated by the interaction of the fragments during the avalanche, rather than by the presence of a fluid (Hungr et al., 2014). The landslides deposit texture of comet 67P resembles the same deposits observed for terrestrial rock avalanche case studies. As outlined in the images (Figure 3), the deposits are mainly composed of boulder fields that have been fragmented during the landslide event.

Generally, the 67P massive deposits are considered the result of a single collapse event (due to the morphology), not ruling out the idea that after the event there could be smaller rock falls. From a morphological point of view, we do not see different overlays of material in the deposit resulting from multiple cliff

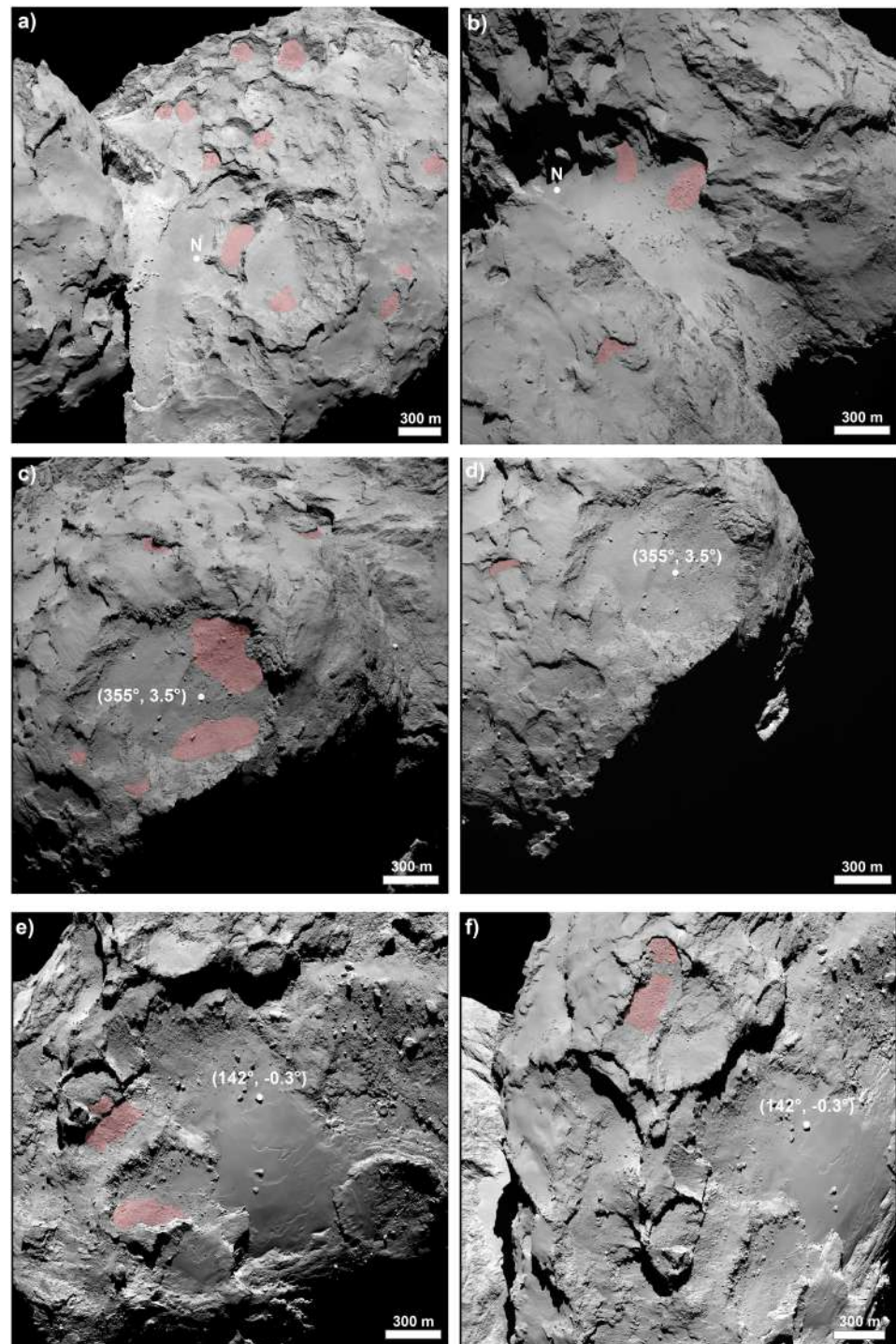


Figure 2. Landslide deposits on the surface of 67P. Landslide accumulation deposits (light red) mapped on the surface of the comet (see El-Maarry et al., 2016, for nomenclature of 67P geological regions). (a) Eleven landslide accumulation deposits located on the body of the comet, in the geological regions of Seth and Ash (NAC_2014-08-08T02.37.34.580Z_ID30_1397549700_F22). (b) Two landslides accumulation deposits located on the neck at the boundary of the Seth and Hapi regions and a landslide located on the head of the comet in the Maat region (NAC_2014-08-22T21.43.27.697Z_ID30_1397549002_F16). (c, d) Six landslides located on the head of the comet in the Hatmehit and Maat regions (NAC_2014-09-02T19.44.22.551Z_ID30_1397549400_F22, NAC_2014-08-23T12.42.54.577Z_ID30_1397549700_F22). (e, f) Five landslide accumulation deposits located on the body of the comet, mainly in the Imhotep and Ash regions (NAC_2014-09-03T03.44.22.640Z_ID30_1397549000_F22, NAC_2014-08-22T18.42.54.669Z_ID30_1397549700_F22). Landslide measurements are given in supporting information Table S1.

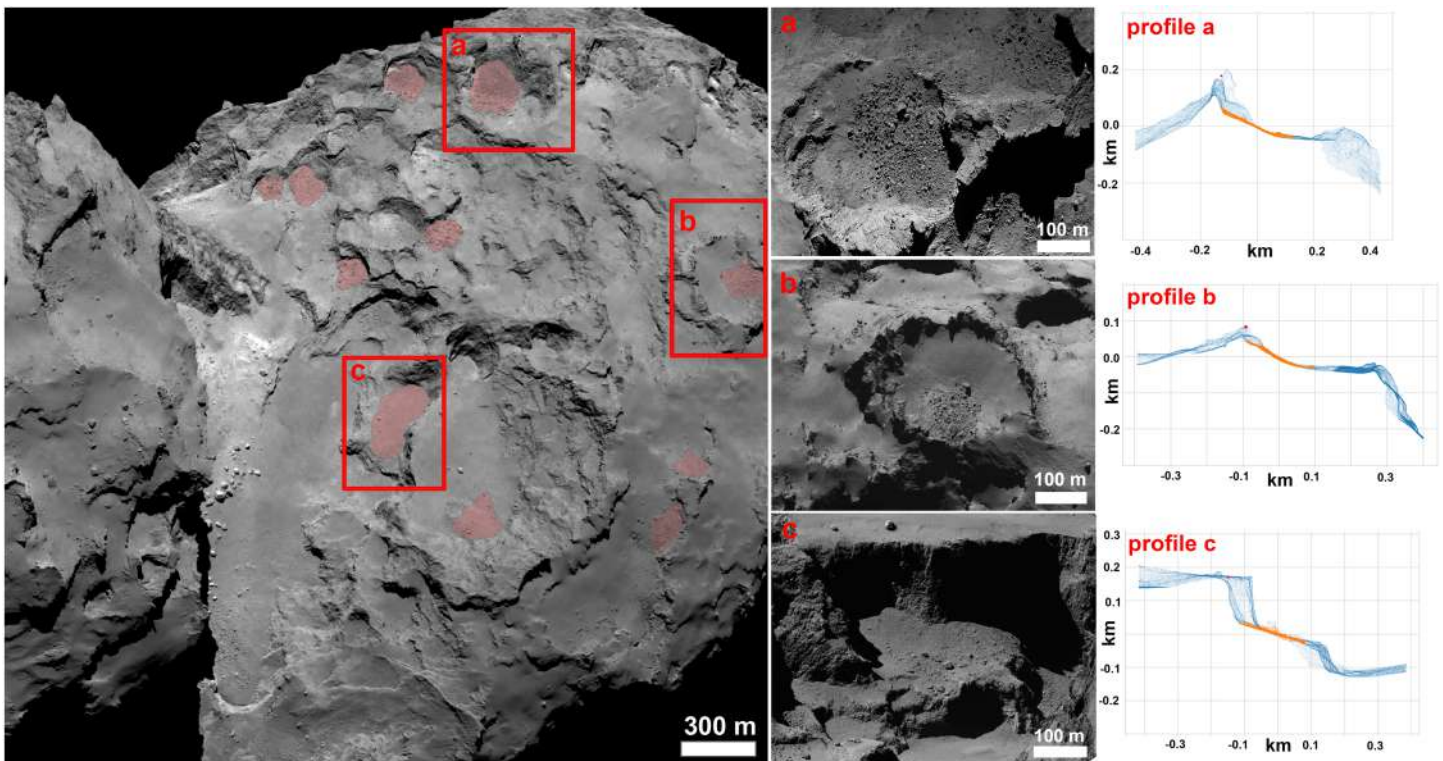


Figure 3. Example of landslides on comet 67P. Three 67P landslide profiles (blue points), where the red dot and the orange dots correspond to the head of the scarp and the deposit extent, respectively. Explanation of the H and L measurements are given in the supporting information. (a) Landslide deposit located in the Seth region. The apparent friction coefficient (H/L) value is equal to 0.83. (b) A landslide located in the Ash region with a H/L value of 0.62. (c) The Aswan cliff collapse (Pajola et al., 2017) consists of blocks with sizes >3 m. The H/L value for Aswan is equal to 0.85.

collapses (despite having extremely high spatial resolution images), but we observe single deposits of material likely resulting from initial events of rock/ice avalanche. A superposition of rock avalanche and rock fall mechanisms is visible in few of the 67P landslides, which may exhibit the character of both failure types (rock avalanche and rock fall). For these landslides, several large fragments are decoupled from the depositing mass, bouncing and rolling away from the deposit in the manner of a fragmental rock fall.

3. Landslide Comparison on Comet 67P and Planetary Bodies

Cometary landslides, first observed and analyzed in detail on 67P, have dimensions that range from tens to hundreds of meters and are small compared to the kilometer-scale landslides observed on other solar system bodies (Brunetti et al., 2014; Legros, 2002; Quantin et al., 2004; Singer et al., 2012; Schmidt et al., 2017).

A pivotal variable to characterize landslides is the ratio of drop height (H) to runout length (L; Heim's ratio; Heim, 1932), which is an approximation for the friction coefficient of the sliding material (Scheidegger, 1973; Hsu, 1975; supporting information). The H/L ratio gives a measurement of the apparent friction angle of the failed materials, and it is equal to the tangent of the slope angle of the line connecting the top of the scarp and the toe of the deposit (Shaller, 1991). Its inverse, L/H, measures the efficiency or mobility of the landslides (McEwen, 1989; Dade & Huppert, 1998; Imre, 2004; Bigot-Cormier & Montgomery, 2007). A more rigorous approach would be to calculate the runout length and drop height based on the center of mass of the landslide (Lucas & Mangeney, 2007; Lucas et al., 2014). However, in absence of other data, the H/L value enables the comparison between geometric features of mass movements on solar system bodies (McEwen, 1989; Singer et al., 2012). A small H/L ratio means that the landslide is capable of travelling for a long distance despite a comparatively small drop height. On Earth and Mars, rock avalanches show a decreasing H/L

with increasing landslide length (or volume; McEwen, 1989; Quantin et al., 2004; Collins & Melosh, 2003). On icy bodies, such as Iapetus and Ceres, H/L scatters in a lower range regardless of length (or volume; Singer et al., 2012; Schmidt et al., 2017). This behavior is consistent with frictional control on runout length but, unlike the terrestrial and Martian linear trends, does not indicate a role for gravity-independent yield strength, such as predicted by Bingham or acoustic fluidization models (Singer et al., 2012).

We reported the details on the H and L measurement in the supporting information. The H was estimated from the head of the scarp to the top of the toe of the corresponding landslide deposit, as performed in previous works (De Blasio, 2011; McEwen, 1989). In addition, thanks to the exploitation of various NAC and WAC high-resolution images, we achieved different view of the same landslide allowing us to better constrain the point from which the material fell down. Then, we consider the shape model of the comet (Preusker et al., 2017) to have the 3-D reconstruction of the region of interest and to correct our inferences for the topography of the comet. In this way, we consider also the gravity vector in measuring the values of H and L. The runout distance measurements were determined along the same line as the drop height. Drop height-measured values range between 53 and 220 m, with the tallest scarp being located in the Seth region. Landslide runout lengths range from 65 to 360 m, with the longest runout observed on the head of the comet in the Hatmehit region. By assuming free fall conditions, and considering that the mean 67P gravity is $2 \times 10^{-4} \text{ m s}^{-2}$ (Preusker et al., 2017), the maximum landslides velocities for the calculated drop heights would be of $0.11\text{--}0.3 \text{ m s}^{-1}$.

Figure 4a shows the H/L values of 67P landslides as a function of the runout length (L), which can be considered a proxy for the volume (Singer et al., 2012). In addition, we compare data with values derived from other solar system bodies. Figure 4b shows a similar comparison for H versus L, highlighting the meter-scale landslide behavior identified on a comet that could not be studied before. The H/L values for 67P do not show a well-defined decreasing trend with increasing L, and they scatter in a range between 0.50 and 0.97 (Figure 4a). Such values are larger than those observed on other solar system bodies, in particular compared to the icy bodies'. This analysis suggests that the falling icy material constituting the comet is characterized by a mechanical behavior that is not comparable to the collapsed ice on other bodies. Indeed, the collapsed icy mass is characterized by a low friction coefficient of the mass favoring its transport over longer distances (Singer et al., 2012). On the contrary, 67P landslides move with high apparent friction coefficient values, which are more comparable with those typically found in avalanches of dry rock on Earth and Mars, with H/L usually exceeding 0.3 (Collins & Melosh, 2003; Hsu, 1975; Quantin et al., 2004).

4. Results and Discussion

4.1. Revealing the Rock-Type Behavior of 67P Landslides

67P landslides have modest-to-high coefficients of friction that significantly differ from those found on icy satellites (Singer et al., 2012; Schmidt et al., 2017). Experiments performed in a microgravity environment (Kleinhans et al., 2011) suggest that lower gravity might produce a reduction of the dynamic repose angle (thus possible longer runouts) because of a larger increase of volume of the released mass and, hence, a lower number of frictional contact points in between the loose material's grains. On the contrary, other work stated that the dynamic repose angle is not a function of gravity (Atwood-Stone & McEwen, 2013). The 67P case seems to be independent on gravity, unless other factors, such as an inherently larger friction coefficient, exert a larger control on the final runout.

Moreover, the material constituting the landslide deposits appears composed of diamicton (Giacomini et al., 2016) with fragmented blocks with a general rocky appearance, deviating from the flow-like morphologies found on icy bodies landslides. On icy satellites, temperature changes due to localized flash heating occur during landslide motion. Evidence for this phenomenon has been found on Iapetus, Callisto, Rhea, and Charon (Singer et al., 2012; Beddingfield et al., 2018). When the temperature of the landslide ice increases, approaching its melting temperature, the friction coefficient decreases, causing material to slide further from its source and creating long runouts. The friction coefficient of water ice is expected to be within the range of 0.15–0.76 (e.g., Durham et al., 1983; Beeman et al., 1988; Schulson & Fortt, 2012): Frictional heating has been shown to decrease these values to 0.29–0.64 for 223 K ice, reaching 0.16 to 0.49 for 263 K ice (Schulson & Fortt, 2012). The mean surface temperature of the comet is between 180 and 230 K (Capaccioni et al.,

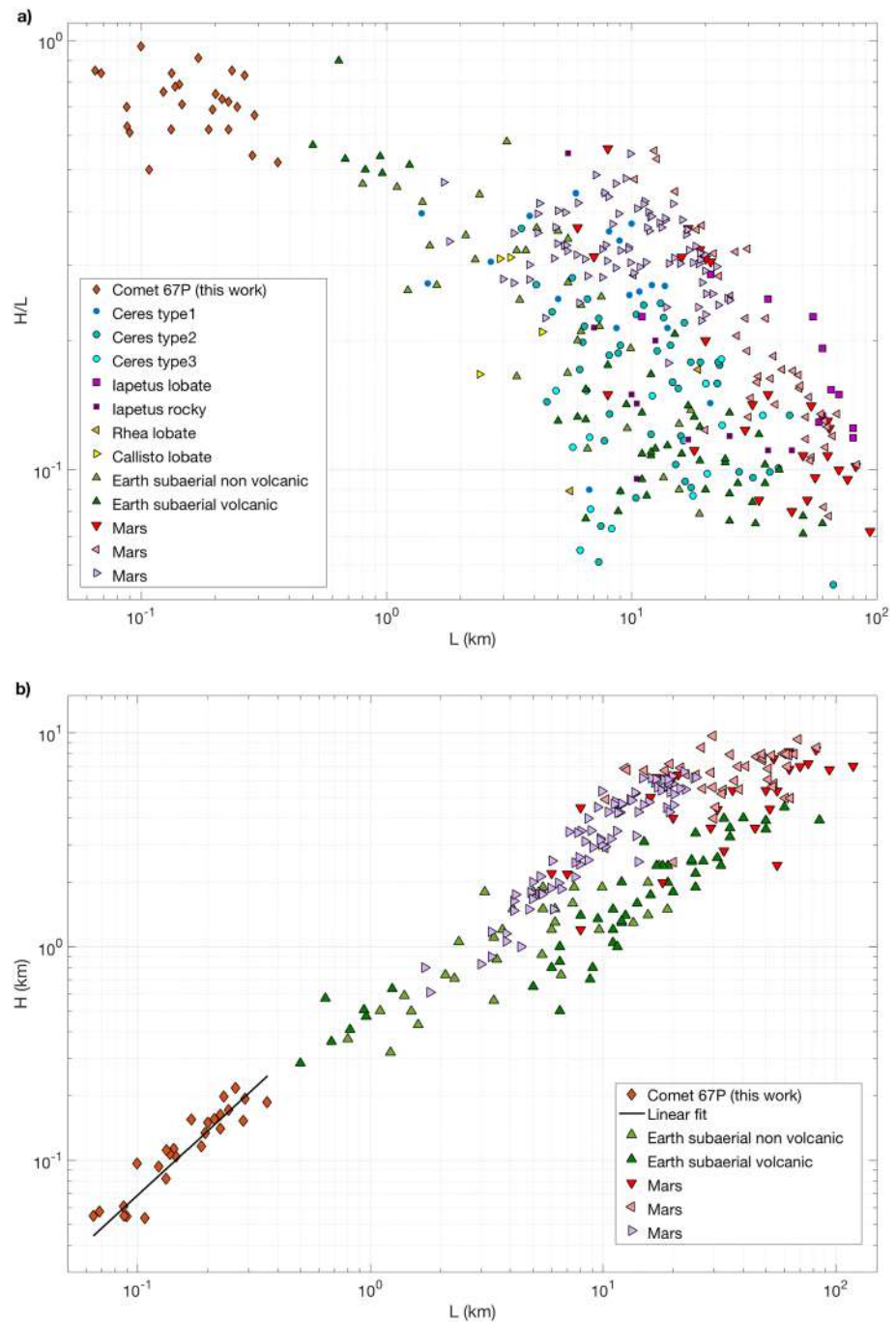


Figure 4. 67P landslides mobility compared to other planetary bodies. (a) The measurements obtained for both rocky bodies, such as terrestrial subaerial landslides (Legros, 2002), Martian landslides in Valles Marineris (pink triangles: Quantin et al., 2004; violet triangles: Brunetti et al., 2014), a data set of earlier Viking measurements (McEwen, 1989; red triangles), and icy bodies, such as debris aprons within craters on Jupiter’s moon Callisto and Saturnian moons Rhea and Iapetus (Singer et al., 2012), three types of landslides identified on Ceres (Schmidt et al., 2017), compared to the 67P landslides identified in this study. (b) Dependence of landslide drop height on runout distance for comet 67P landslides compared to the Earth and Mars landslide dataset reported in (a). The black line shows the relationship obtained through linear fitting between L and H. For the specific case of Mars, the relationship reported in Brunetti et al. (2014) is $H_{\text{drop}} = 0.29 L_{\text{runout}}$ implying an apparent friction angle of 14°. In the comet case, the apparent friction angle is about 34° (relationship of $H_{\text{drop}} = 0.68 L_{\text{runout}}$), suggesting a higher internal friction of the material.

2015) and the specific potential energy released during an avalanche on 67P, that is, gH , ranges from 0.01 to 0.04 J kg^{-1} . This is clearly not enough to heat the ice (making it slippery or melting it, as in Iapetus case) and consequently decrease the friction of the collapsed mass.

In summary, the apparent friction coefficients on 67P derived from this analysis are comparable to landslides characterizing water ice in the absence of frictional heating. More likely, the values are comparable to the one generally applied to static or sliding friction of dry rock (see Byerlee law; Jaeger et al., 2009). Given that the 67P high friction coefficients are comparable, or even exceed, those found on Earth dry landslides (Legros, 2002), this implies a mechanically rocky-type behavior for the cometary material.

The texture of the landslide deposits, suggesting fragmentation during the avalanche, supports this interpretation. Hence, although the high porosity (75–97%; Kofman et al., 2015) and low density of 67P might suggest poorly welded materials, the texture and morphology of its landslides reveal a clear brittle behavior. This is indeed testified by the ubiquitous presence of fractures on all the cliffs from which landslides formed (thermal cracking has been suggested to be one of the triggers mechanisms of a cliff collapse; Pajola et al., 2017) meaning that the collapsed material of 67P is cohesive and well consolidated once detached. The calculated mean landslide apparent friction angle of 34° is considerably higher than the values (14°) reported for fractured rock mass in other context (Quantin et al., 2004; Brunetti et al., 2014) and more comparable to those of pristine rocks such as sandstones, siltstones, gneisses, and slates (from 27 to 34°), or basalts, granites, and limestones (from 34° to 40° ; Wyllie & Mah, 2005). This comparison indicates that the cometary material is characterized by a high to medium internal friction coefficient.

All these results make 67P a very peculiar object, mainly composed by ices and refractory materials, but characterized by rocky-type properties rather than icy-type characteristics. The rocky-type behavior we highlight with this work does not mean that the material constituting comet 67P is dense as rock, as the mean bulk density of 537.8 kg m^{-3} points out (Preusker et al., 2017). Nevertheless, we observed that 67P material is highly fractured, as well as it did not largely compress, as in the case of rolling boulders (Vincent et al., 2019). On Earth, such properties generally belong to material that cannot be considered fluffy. Despite that, we still do not have a definitive, undisputable proof regarding 67P composition, and for this reason we have to rely for our statement on 67P's H/L values. Indeed, such values are in some cases more similar to Earth dry volcanic landslides, that is, strengthening the idea that cometary material under 67P low gravity behaves like terrestrial rock.

4.2. Implication for Different Volatile Content in 67P

The variation of friction coefficients measured on 67P is not due to different inclination of the slopes from which material falls since the gravitational slopes of the considered cliffs are all similar (supporting information). We therefore suggest that the range of H/L values of 67P (between 0.50 and 0.97) can be explained by variations in the volatile content within the top few meters of the comet surface. The surface of comet 67P is considered heterogeneous from a compositional perspective. Observations at visible-infrared (VIS-IR) wavelengths performed by the VIRTIS (Coradini et al., 2007; Visible, Infrared and Thermal Imaging Spectrometer) and OSIRIS instruments have revealed a surface covered by low-albedo materials (Capaccioni et al., 2015; Fornasier et al., 2015), characterized by the presence of refractory and semivolatile organics and dark opaque phases (Quirico et al., 2016). Several local bright spots have been interpreted as exposures of water ice (De Sanctis et al., 2015; Fornasier et al., 2016; Oklay et al., 2017), in addition to the presence of carbon dioxide ice (Filacchione et al., 2016). While approaching perihelion, the increasing level of activity partially removed parts of the overlying refractory mantling material leading to the exposure of the underlying ice-rich layers that soon sublimated and caused changes in the surface appearance (Fornasier et al., 2016).

The different morphologies observed on 67P are hypothesized to be the result of regional to local variations of the volatile content (Vincent et al., 2015), differently processed by the diurnal and seasonal insolation changes while approaching perihelion. Our observations support this interpretation, suggesting that different H/L values of landslides on 67P can be expression of different volatile contents within the collapsed material. Indeed, volatiles that are released by sublimating cliffs during the gravitational event might facilitate longer landslides runouts length through overpressure at the sliding surface. We point out that other dissipative processes, possibly sublimation-driven, could in principle be at the origin of the unusually high H/L

values, but they are of difficult evaluation due to the lack of previous studies on cometary landslides. For this reason, we limited our interpretation to factors that are known to exert a strong control on runout distances and are common to any landslide on all planetary bodies.

Therefore, we indicate that lower values of H/L are representative of a higher concentration of volatile transiting in longer landslides runouts, while higher H/L values reflect a smaller content of volatiles hence resulting in shorter landslide runouts. These values imply that for comets, different H/L values can be used as an indicator of the different localized volatile content that fosters the material to slide nearer or farther from the scarp face.

5. Conclusion

The detailed characterization and analysis of landslides on 67P widens the data set of the solar system landslides considering meter-scale case studies that were not analyzed before on other planetary bodies. By assuming the height to runout length as an approximation for the friction coefficient of landslide material, we find that on comet 67P, this ratio falls between 0.50 and 0.97. Given that the 67P high friction coefficients are comparable, or even exceed, those found on Earth dry landslides (Legros, 2002), this implies a mechanically rocky-type behavior for the cometary material. Our findings reject the idea that comets are fluffy aggregates; instead, they are characterized by consolidated surfaces.

Landslides on 67P reveal a clear rocky-type behavior for cometary material that, once collapsed, assumes a rock avalanche mobilization associated to relatively high friction coefficients. This behavior agrees with the refractory to ice ratio estimated from grains ejected from 67P (Fulle et al., 2019). In addition, the considerable variability of H/L values among the different landslides suggests that different volatile contents of the detached mass play a fundamental role on the gravitational process and final runout, hence being a general indicator for the subsurface cometary heterogeneities.

Acknowledgments

OSIRIS was built by a consortium of the Max-Planck-Institut für Sonnensystemforschung, in Göttingen, Germany, CISAS-University of Padova, Italy, the Laboratoire d'Astrophysique de Marseille, France, the Instituto de Astrofísica de Andalucía, CSIC, Granada, Spain, the Research and Scientific Support Department of the European Space Agency, Noordwijk, The Netherlands, the Instituto Nacional de Técnica Aeroespacial, Madrid, Spain, the Universidad Politécnica de Madrid, Spain, the Department of Physics and Astronomy of Uppsala University, Sweden, and the Institut für Datentechnik und Kommunikationsnetze der Technischen Universität Braunschweig, Germany. The support of the national funding agencies of Germany (DLR), Italy (ASI), France (CNES), Spain (MEC), Sweden (SNSB), and the ESA Technical Directorate is gratefully acknowledged. We thank the ESA teams at ESAC, ESOC, and ESTEC for their work in support of the Rosetta mission. We made use of ArcMap 10.3.1 and Matlab software to perform our analysis. All the images analyzed during the current study and the 3-D 67P shape model are available in the ESA-PSA repository (<https://archives.esac.esa.int/psa>). The data archiving that support the findings of this study are on the following Zenodo repository, doi: 10.5281/zenodo.3516279.

References

- Atwood-Stone, C., & McEwen, S. A. (2013). Avalanche slope angles in low-gravity environments from active Martian sand dunes. *Geophysical Research Letters*, *40*, 2929–2934. <https://doi.org/10.1002/grl.50586>
- Bart, G. D., et al. (2007). Comparison of small lunar landslides and Martian gullies. *Icarus*, *187*, 417–421.
- Beddingfield, C. B., Beyer, R. A., Singer, K., Nimmo, F., McKinnon, W. B., Moore, J. M., et al. (2018). Landslides in the Serenity Chasma region, Charon. *49th Lunar Planet. Sci.*, abs. #2083.
- Beeman, M., Durham, W. B., & Kirby, S. H. (1988). Friction of ice. *Journal of Geophysical Research*, *93*, 7625–7633.
- Bigot-Cormier, F., & Montgomery, D. R. (2007). Valles Marineris landslides: Evidence for a strength limit to Martian relief? *Earth and Planetary Science Letters*, *260*, 179–186.
- Britt, D. T., Boice, D. C., Buratti, B. J., Campins, H., Nelson, R. M., Oberst, J., et al. (2004). The morphology and surface processes of Comet 19/P Borrelly. *Icarus*, *167*(1), 45–53. <https://doi.org/10.1016/j.icarus.2003.09.004>
- Brunetti, M. T., Guzzetti, F., Cardinali, M., Fiorucci, F., Santangelo, M., Mancinelli, P., et al. (2014). Analysis of a new geomorphological inventory of landslides in Valles Marineris, Mars. *Earth and Planetary Science Letters*, *405*, 156–168. <https://doi.org/10.1016/j.epsl.2014.08.025>
- Capaccioni, F., Coradini, A., Filacchione, G., Erard, S., Arnold, G., Drossart, P., et al. (2015). The organic-rich surface of comet 67P/Churyumov-Gerasimenko as seen by VIRTIS/Rosetta. *Science*, *347*, 628.
- Collins, G. S., & Melosh, H. J. (2003). Acoustic fluidization and the extraordinary mobility of sturzstroms. *Journal of Geophysical Research*, *108*(B10), 2473. <https://doi.org/10.1029/2003JB002465>
- Coradini, A., Capaccioni, F., Drossart, P., Arnold, G., Ammannito, E., Angrilli, F., et al. (2007). Virtis: An imaging spectrometer for the Rosetta Mission. *Space Science Reviews*, *128*(1–4), 529–559. <https://doi.org/10.1007/s11214-006-9127-5>
- Crosta, G. B., Frattini, P., Valbuzzi, E., & de Blasio, F. V. (2018). Introducing a new inventory of large Martian landslides. *Earth and Space Science*, *5*(4), 89–119. <https://doi.org/10.1002/2017EA000324>
- Cruden, D. M., & Varnes, D. J. (1996). *Landslides: Investigation and mitigation*. Chapter 3-Landslide types and processes. Transportation research board special report, (247).
- Dade, W. B., & Huppert, H. E. (1998). Long-runout rockfalls. *Geology*, *26*, 803–806.
- De Blasio, F. V. (2011). Introduction to the physics of landslides: Lecture notes on the dynamics of mass wasting. Springer Science & Business Media.
- De Sanctis, M. C., Capaccioni, F., Ciarniello, M., Filacchione, G., Formisano, M., Mottola, S., et al. (2015). The diurnal cycle of water ice on comet 67P/Churyumov-Gerasimenko. *Nature*, *525*(7570), 500–503. <https://doi.org/10.1038/nature14869>
- Durham, W. B., Heard, H. C., & Kirby, S. H. (1983). Experimental deformation of polycrystalline H₂O ice at high pressure and low temperature: Preliminary results. *Journal of Geophysical Research*, *88*, S01.
- El-Maarry, M. R., Thomas, N., Gracia-Berná, A., Pajola, M., Lee, J.-C., Massironi, M., et al. (2016). Regional surface morphology of comet 67P/Churyumov-Gerasimenko from Rosetta/OSIRIS images: The southern hemisphere. *Astronomy and Astrophysics*, *593*, A110. <https://doi.org/10.1051/0004-6361/201628634>
- Filacchione, G., Raponi, A., Capaccioni, F., Ciarniello, M., Tosi, F., Capria, M. T., et al. (2016). Seasonal exposure of carbon dioxide ice on the nucleus of comet 67P/Churyumov-Gerasimenko. *Science*, *354*(6319), 1563–1566. <https://doi.org/10.1126/science.aag3161>

- Fornasier, S., Hasselmann, P. H., Barucci, M. A., Feller, C., Besse, S., Leyrat, C., et al. (2015). Spectrophotometric properties of the nucleus of comet 67P/Churyumov-Gerasimenko from the OSIRIS instrument onboard the ROSETTA spacecraft. *Astronomy and Astrophysics*, 583, A30. <https://doi.org/10.1051/0004-6361/201525901>
- Fornasier, S., Mottola, S., Keller, H. U., Barucci, M. A., Davidsson, B., Feller, C., et al. (2016). Rosetta's comet 67P/Churyumov-Gerasimenko sheds its dusty mantle to reveal its icy nature. *Science*, 354(6319), 1566–1570. <https://doi.org/10.1126/science.aag2671>
- Fulle, M., Blum, J., Green, S. F., Gundlach, B., Herique, A., Moreno, F., et al. (2019). The refractory-to-ice mass ratio in comets. *Monthly Notices of the Royal Astronomical Society*, 482(3), 3326–3340. <https://doi.org/10.1093/mnras/sty2926>
- Giacomini, L., Massironi, M., el-Maarry, M. R., Penasa, L., Pajola, M., Thomas, N., et al. (2016). Geologic mapping of the Comet 67P/Churyumov-Gerasimenko's northern hemisphere. *Monthly Notices of the Royal Astronomical Society*, 462(Suppl 1), S352–S367. <https://doi.org/10.1093/mnras/stw2848>
- Heim, A. (1932). Bergsturz und menschenleben (No. 20). Fretz & Wasmuth.
- Hsu, K. J. (1975). Catastrophic debris streams (sturzstroms) generated by rockfalls. *Geological Society of America Bulletin*, 86, 129–140.
- Hungr, O., Leroueil, S., & Picarelli, L. (2014). The Varnes classification of landslide types, an update. *Landslides*, 11(2), 167–194.
- Imre, B. (2004). Numerical slope stability simulations of the northern wall of eastern Candor Chasma (Mars) utilizing a distinct element method. *Planetary and Space Science*, 52(14), 1303–1319.
- Jaeger, J. C., Cook, N. G., & Zimmerman, R. (2009). *Fundamentals of rock mechanics*. John Wiley & Sons.
- Keller, H. U., Barbieri, C., Lamy, P., Rickman, H., Rodrigo, R., Wenzel, K. P., et al. (2007). OSIRIS—The scientific camera system onboard Rosetta. *Space Science Reviews*, 128(1-4), 433–506. <https://doi.org/10.1007/s11214-006-9128-4>
- Kleinhans, M. G., Markies, H., de Vet, S. J., in't Veld, A. C., & Postema, F. N. (2011). Static and dynamic angles of repose in loose granular materials under reduced gravity. *Journal of Geophysical Research*, 116, E11004. <https://doi.org/10.1029/2011JE003865>
- Kofman, W., Herique, A., Barbin, Y., Barriot, J. P., Ciarletti, V., Clifford, S., et al. (2015). Properties of the 67P/Churyumov-Gerasimenko interior revealed by CONSERT radar. *Science*, 349(6247), aab0639. <https://doi.org/10.1126/science.aab0639>
- Lai, I. L., Ip, W.-H., Su, C.-C., Wu, J.-S., Lee, J.-C., Lin, Z.-Y., et al. (2017). Gas outflow and dust transport of comet 67P/Churyumov-Gerasimenko. *Monthly Notices of the Royal Astronomical Society*, 462(Suppl_1), S533–S546.
- Legros, F. (2002). The mobility of long-runout landslides. *Engineering Geology*, 63, 301–331.
- Lucas, A., & Mangeney, A. (2007). Mobility and topographic effects for large Valles Marineris landslides on Mars. *Geophysical Research Letters*, 34, L10201. <https://doi.org/10.1029/2007GL029835>
- Lucas, A., Mangeney, A., & Ampuero, J. P. (2014). Frictional velocity-weakening in landslides on Earth and on other planetary bodies. *Nature Communications*, 5.
- Lucchitta, B. K. (1987). Valles Marineris, Mars Wet debris flows and ground ice. *Icarus*, 72, 411–429.
- Malin, M. C. (1992). Mass movements on Venus—Preliminary results from Magellan cycle 1 observations. *Journal of Geophysical Research*, 97, 16,337–16,352.
- Malin, M. C., & Dzurisin, D. (1978). Modification of fresh crater landforms: evidence from the Moon and Mercury. *Journal of Geophysical Research*, 83, 233–243.
- McEwen, A. S. (1989). Mobility of large rock avalanches: Evidence from Valles Marineris. *Mars. Geology*, 17, 1111–1114.
- Moore, J. M., Asphaug, E., Morrison, D., Spencer, J. R., Chapman, C. R., Bierhaus, B., et al. (1999). Mass movement and landform degradation on the icy Galilean satellites: Results of the Galileo nominal mission. *Icarus*, 140(2), 294–312. <https://doi.org/10.1006/icar.1999.6132>
- Oklay, N., Mottola, S., Vincent, J. B., Pajola, M., Fornasier, S., Hviid, S. F., et al. (2017). Long-term survival of surface water ice on comet 67P. *Monthly Notices of the Royal Astronomical Society*, 469(Suppl_2), S582–S597. <https://doi.org/10.1093/mnras/stx2298>
- Otto, K. A., Jaumann, R., Krohn, K., Matz, K.-D., Preusker, F., Roatsch, T., et al. (2013). Mass-wasting features and processes in Vesta's south polar basin Rheasilvia. *Journal of Geophysical Research*: Planets, 118, 2279–2294. <https://doi.org/10.1002/2013JE004333>
- Pajola, M., Höfner, S., Vincent, J. B., Oklay, N., Scholten, F., Preusker, F., et al. (2017). The pristine interior of comet 67P revealed by the combined Aswan outburst and cliff collapse. *Nature Astronomy*, 1(5), 0092. <https://doi.org/10.1038/s41550-017-0092>
- Pajola, M., Lucchetti, A., Vincent, J. B., Oklay, N., el-Maarry, M. R., Bertini, I., et al. (2016). The southern hemisphere of 67P/Churyumov-Gerasimenko: Analysis of the preperihelion size-frequency distribution of boulders ≥ 7 m. *Astronomy and Astrophysics*, 592, L2. <https://doi.org/10.1051/0004-6361/201628887>
- Pajola, M., Vincent, J. B., Güttler, C., Lee, J. C., Bertini, I., Massironi, M., et al. (2015). Size-frequency distribution of boulders ≥ 7 m on comet 67P/Churyumov-Gerasimenko. *Astronomy and Astrophysics*, 583, A37. <https://doi.org/10.1051/0004-6361/201525975>
- Pike, R. J. (1988). The geometric signature: Quantifying landslide-terrain types from digital elevation models. *Mathematical Geology*, 20(5), 491–511.
- Preusker, F., Scholten, F., Matz, K. D., Roatsch, T., Hviid, S. F., Mottola, S., et al. (2017). The global meter-level shape model of comet 67P/Churyumov-Gerasimenko—Stereo-photogrammetric analysis of Rosetta/OSIRIS image data. *Astronomy and Astrophysics*, 607, L1. <https://doi.org/10.1051/0004-6361/201731798>
- Preusker, F., Scholten, F., Matz, K. D., Roatsch, T., Willner, K., Hviid, S. F., et al. (2015). Shape model, reference system definition, and cartographic mapping standards for comet 67P/Churyumov-Gerasimenko—Stereo-photogrammetric analysis of Rosetta/OSIRIS image data. *Astronomy and Astrophysics*, 583, A33. <https://doi.org/10.1051/0004-6361/201526349>
- Quantin, C., Allemand, P., & Delacourt, C. (2004). Morphology and geometry of Valles Marineris landslides. *Planetary and Space Science*, 52, 1011–1022.
- Quirico, E., Moroz, L. V., Schmitt, B., Arnold, G., Faure, M., Beck, P., et al. (2016). Refractory and semi-volatile organics at the surface of comet 67P/Churyumov-Gerasimenko: Insights from the VIRTIS/Rosetta imaging spectrometer. *Icarus*, 272, 32–47. <https://doi.org/10.1016/j.icarus.2016.02.028>
- Scheidegger, A. E. (1973). On the prediction of the reach and velocity of catastrophic landslides. *Rock Mechanics*, 5, 231–236.
- Schenk, P. M., & Bulmer, M. H. (1998). Origin of mountains on Io by thrust faulting and large-scale mass movements. *Science*, 279(5356), 1514–1517. <https://doi.org/10.1126/science.279.5356.1514>
- Schmidt, B. E., Hughson, K. H. G., Chilton, H. T., Scully, J. E. C., Platz, T., Nathues, A., et al. (2017). Geomorphological evidence for ground ice on dwarf planet Ceres. *Nature Geoscience*, 10, 338–343.
- Schulson, E. M., & Fortt, A. L. (2012). Friction of ice on ice. *Journal of Geophysical Research*, 117, B12204. <https://doi.org/10.1029/2012JB009219>
- Shaller, P. J. (1991). Analysis and implications of large Martian and terrestrial landslides. Dissertation (PhD), California Institute of Technology.
- Shingareva, T. V., & Kuzmin, R. O. (2001). Mass-wasting processes on the surface of Phobos. *Solar System Research*, 35, 431–443.

- Sierks, H., Barbieri, C., Lamy, P. L., Rodrigo, R., Koschny, D., Rickman, H., et al. (2015). On the nucleus structure and activity of comet 67P/Churyumov-Gerasimenko. *Science*, *347*, 388.
- Singer, K. N., McKinnon, W. B., Schenk, P. M., & Moore, J. M. (2012). Massive ice avalanches on Iapetus mobilized by friction reduction during flash heating. *Nature Geoscience*, *5*, 574–578.
- Steckloff, J. K., Graves, K., Hirabayashi, M., Melosh, H. J., & Richardson, J. E. (2016). Rotationally induced surface slope-instabilities and the activation of CO₂ activity on comet 103P/Hartley 2. *Icarus*, *272*, 60–69.
- Steckloff, J. K., & Samarasingha, N. H. (2018). The sublimative torques of Jupiter Family Comets and mass wasting events on their nuclei. *Icarus*, *312*, 172–180.
- Thomas, N., Sierks, H., Barbieri, C., Lamy, P. L., Rodrigo, R., Rickman, H., et al. (2015). The morphological diversity of comet 67P/Churyumov-Gerasimenko. *Science*, *347*(6220), aaa0440. <https://doi.org/10.1126/science.aaa0440>
- Vincent, J. B., Birch, S., Hayes, A., Zacny, K., Oklay, N., Cambianica, P. (2019). Bouncing boulders on comet 67P, EPSC-DPS Joint Meeting 2019.
- Vincent, J. B., Bodewits, D., Besse, S., Sierks, H., Barbieri, C., Lamy, P., et al. (2015). Large heterogeneities in comet 67P as revealed by active pits from sinkhole collapse. *Nature*, *523*(7558), 63–66. <https://doi.org/10.1038/nature14564>
- Vincent, J. B., Hviid, S. F., Mottola, S., Kuehrt, E., Preusker, F., Scholten, F., et al. (2017). Constraints on cometary surface evolution derived from a statistical analysis of 67P's topography. *Monthly Notices of the Royal Astronomical Society*, *469*(Suppl_2), S329–S338. <https://doi.org/10.1093/mnras/stx1691>
- Wyllie, D. C., & Mah, C. W. (2005). *Rock slope engineering*. Spon Press, Taylor and Francis Group.
- Xiao, Z., Zeng, Z., Ding, N., & Molaro, J. (2013). Mass wasting features on the Moon—How active is the lunar surface? *Earth and Planetary Science Letters*, *376*, 1–11.